

# Searching for MACHOs in Galaxy Clusters

Geraint F. Lewis

*Anglo-Australian Observatory, P.O. Box 296, Epping, NSW 1710, Australia*

`gfl@aaoepp.aao.gov.au`

Rodrigo A. Ibata

*Max-Planck Institut für Astronomie, Königstuhl 17, D-69117 Heidelberg, Germany*

`ribata@mpia-hd.mpg.de`

J. Stuart B. Wyithe

*School of Physics, University of Melbourne, Parkville, Vic 3052, Australia &*

*Princeton University Observatory, Peyton Hall, Princeton, NJ 08544, USA*

`swyithe@astro.princeton.edu`

## ABSTRACT

If cluster dark matter is in the form of compact objects it will introduce fluctuations into the light curves of distant sources. Current searches for MACHOs in clusters of galaxies focus on monitoring quasars behind nearby systems. This paper considers the effect of such a compact population on the surface brightness distribution of giant gravitationally lensed arcs. As the microlensing optical depth is significant in these clusters, the expected fluctuations are substantial and are observable. Focusing on the giant arc seen in Abell 370, we demonstrate that several ‘extreme’ events would be visible in a comparison of HST observations at two epochs. Utilizing NGST, long term monitoring should reveal a ubiquitous twinkling of brightness over the surface of the arcs.

*Subject headings:* galaxies: clusters: general – gravitational lensing – dark matter

## 1. Introduction

After many years of searching, the nature of dark matter still eludes us. Over the last decade, however, programs searching for microlensing variability in stars in the Magellanic Clouds have revealed a population of compact objects in front of the LMC (Afonso *et al.* 1999; Alcock *et al.* 2000a). The EROS team have used their observations to place an upper limit of 10% of the mass fraction in MACHOs in the Galactic halo (Lasserre *et al.* 2000), while the MACHO team interprets their data as providing evidence of a significant fraction, perhaps 20%. The recent discovery of nearby cold, high proper motion, hydrogen atmosphere white dwarfs appears to support the

latter interpretation (Ibata *et al.* 2000; Hodgkin *et al.* 2000). These results are complicated by fact that views towards the Galactic Bulge appear to be overdense in compact objects (Alcock *et al.* 2000b), suggesting that the Galactic Halo is clumped (c.f. Klypin *et al.* 1999) and our view towards the Magellanic Clouds simply represents an underdense line-of-sight. Currently, therefore, the true fraction of the Galactic Halo composed of compact objects is uncertain.

Galaxy clusters represent the largest bound accumulations of matter in the Universe, and a number of lines of evidence, including kinematic (Bird, Dickey & Salpeter 1993), X-ray (Henry *et al.* 1993) and gravitational lensing (Kneib *et al.*

1993) studies, indicate that they must possess a substantial quantity of dark matter. In this paper we address the question of what would be the observational consequences if this dark matter were also composed of compact objects.

An approach to test the nature of cluster dark matter was recently suggested by Walker & Ireland (1995) and Tadros, Warren & Hewett (1998; 2000). As with compact matter in the Galactic Halo, MACHOs in clusters are expected to introduce brightness fluctuations in background sources, and this is searched for in a monitoring program of  $\sim 600$  quasars behind the Virgo cluster. While initial results are promising, the vicinity of the Virgo cluster means that the microlensing optical depth is small ( $\sim 0.001$ ) and induced fluctuations are relatively rare. The optical depth can be increased by changing the lensing geometry and considering clusters at higher redshift. With this, however, it is difficult to identify a substantial number of background quasars without greatly increasing the number of clusters to be monitored. The problem is also compounded by the difficulty of distinguishing microlensing-induced quasar variability from intrinsic mechanisms.

Lewis & Iбата (2000) addressed the question of what effect a cosmological distribution of compact objects would have on the surface brightness distributions of galaxies at  $z < 0.5$ . While the microlensing optical depth is quite small ( $\sigma \lesssim 0.04$ ), the resulting low-level fluctuations,  $\sim 2\%$ , are observable. In this paper we extend this analysis to the view of distant galaxies observed through galaxy clusters whose dark matter is composed of MACHOs. The ideal targets are the giant gravitationally lensed arcs. Focusing on these systems ensures that the column density of matter through the cluster is substantial, resulting in an optical depth near unity; this vastly exceeds ‘self-lensing’, with an optical depth of only  $\sim 10^{-5}$ , where MACHOs microlens galaxies within the cluster (Gould 1995). Potential sources abound, as giant arcs and extended images have been identified in more than thirty clusters (e.g Fort & Mellier 1994). As the induced variability will be searched for on a pixel-by-pixel basis, each extended image presents a large number of resolution elements which can be viewed as separate sources, far outweighing the potential number of background quasars.

In Section 2 we outline the numerical approach we adopt to tackle this problem, focusing on the simulation of microlensing light curves. As an illustration of the efficiency of microlensing as a mechanism for introducing variability, we present in section 3 a case study of the giant arc seen in the cluster Abell 370. This section also discusses the observational considerations for a monitoring program of giant arcs. The conclusions to this study are presented in Section 4.

## 2. Method

In examining microlensing of sources in the Magellanic Clouds, the goal is to identify the variation in brightness of a single star as a compact object passes in front of it. Considering instead microlensing towards more distant sources, individual stars can no longer be resolved and induced variations are identified against an unresolved stellar background. Termed ‘pixel-lensing’ (e.g. Crofts 1992), the magnification of a star results in the increase of flux in an individual resolution element, and hence appears as a fluctuation in the surface brightness of a source. Employing an efficient technique called ‘Difference Imaging’, searches for such fluctuations have recently proved fruitful with the identification of microlensing variability towards the Galactic Bulge and M31 (Alcock et al. 1999a, 1999b; Ansari et al. 1999).

In a similar vein, observations of gravitationally lensed giant arcs do not resolve individual stars, rather each pixel over an arc represents the summed flux from a population of stars. As stars in this population are magnified due to gravitational microlensing by compact objects in the foreground cluster, the apparent surface brightness of the pixels will be seen to fluctuate. It is important to note that at the substantial optical depths considered in this paper, each star in the population will be subject to microlensing and so the overall light curve seen will be the sum of the individual fluctuations of each star. This differs substantially from pixel lensing in the local group, where the optical depth is small and at most only a small number of stars are significantly microlensed at any instant.

In simulating the expected variability, the following procedure is adopted; firstly, for a particular set of microlensing parameters, a large cat-

atalogue of light curves,  $\mu_i(t)$ , are generated. A population of stars,  $S_i$ , is randomly selected such that the total luminosity of the population is  $L_{POP} = \Sigma L(S_i)$ . Each star is used to normalize a light curve selected from the catalogue to produce a microlensed view of the star. These individual light curves are then combined to produce a total microlensed light curve for the entire stellar population,  $M(t) = \Sigma \mu_i(t) L(S_i)$ . As a consistency check, the mean luminosity of the resultant light curves must equal  $\langle \mu_{th} \rangle L_{POP}$ , where  $\langle \mu_{th} \rangle$  is the mean magnification of the arc induced by the macrolensing model of the cluster. Typically, stellar luminosity functions increase at fainter magnitudes, implying that populations are dominated, in number, by low luminosity stars. Such faint stars, even if substantially lensed, will not significantly contribute to the final light curve. Hence, for any star for which  $\mu_{max} L(S_i) / \langle \mu_{th} \rangle L_{POP} < 0.005$ , where  $\mu_{max}$  is taken to be 70, the contribution to the final light curve is taken as uniform and equal to  $\langle \mu_{th} \rangle L(S_i)$ ; such an approach reduces the required numerical calculations in constructing a light curve. As with Lewis & Ibata (2000), we adopt the stellar luminosity function as determined by Jahreiß & Wielen (1997).

An efficient method of generating high optical depth microlensing light curves for a point-like source is employed (Witt 1993; Lewis, Miralda-Escudé, Richardson & Wambsganss 1993). This approach treats the source trajectory as a line of infinite extent, ensuring that it is numerically simple to find all the microlensed images with a contour following algorithm. This guarantees that the light curve is not lacking flux due to ‘undiscovered’ images. The efficiency allows large samples of light curves to be generated, the basis for a number of extensive statistical studies (Lewis & Irwin 1995; Lewis & Irwin 1996; Wyithe & Webster 1999; Wyithe, Webster & Turner 1999,2000).

While the approach is straight-forward, the volume of potential parameter space is very large and a full examination of this is beyond the scope of this paper, and a more extensive study will be presented elsewhere. As an illustration of the efficacy of microlensing on introducing variability into surface brightness distributions, we now focus on the spectacular giant arc in Abell 370.

### 3. Case Study: A370

At a redshift of  $z = 0.37$ , the rich galaxy cluster Abell 370 possesses several giant gravitationally lensed arcs (Soucail et al. 1987). Utilizing their spatial extent, detailed modeling of the mass distribution of Abell 370 has been undertaken (Kneib et al 1993; Abdelsalam et al. 1998), confirming the binary nature of the cluster. The most prominent giant arc is over 20 arcsecs in extent and has a spectroscopic redshift of  $z = 0.724$  (Soucail et al. 1988). Examining the models for the mass distribution in Abell 370 in the vicinity of this giant arc, we choose a fiducial model with an optical depth of  $\sigma = 0.6$  and shear of  $\gamma = 0.2$ . This results in a mean magnification of  $\langle \mu_{th} \rangle = 8.33$ .

#### 3.1. Light Curves

A large sample of light curves was generated using the above parameter set and combined with the stellar luminosity function to produce the light curves of an entire population as outlined in Section 2. The source trajectory is aligned with the shear, although simple scaling relations to other shear orientations exist (Lewis & Irwin 1995). Each lens has a mass of  $1M_{\odot}$ .

Several light curves of these are presented in Figure 1 for stellar populations of  $L_{POP} = 10^4, 10^5, 10^6$  and  $10^7 L_{\odot}$ ; these numbers represent the intrinsic luminosity of the population, the observed value is  $L_{Obs} = \langle \mu_{th} \rangle L_{POP}$ . The abscissa is in units of Einstein radii for a solar mass star; this is related to a time scale, as explained below. The light curves display the complex variability of high optical depth microlensing. At low optical depths, the light curves would consist of solitary events due to individual microlenses. While these can be used to directly infer microlensing parameters, they occur very rarely and low optical depth light curves are extremely quiescent. With the rich structure seen in the light curves of Figure 1, the details of the microlensing can be determined in a statistical sense (e.g. Lewis & Irwin 1996).

In examining the light curves in Figure 1 it is apparent that the degree of variability drops as the total luminosity is increased, with populations of  $10^4 L_{\odot}$  displaying rapid variations of 10-20% on scales much less than an Einstein radius, while the light curves for populations of  $10^7 L_{\odot}$  appear essentially flat with only small scale variability. This

is due to the fact that even a strongly lensed, very luminous star can contribute only a small amount to the total luminosity of a stellar population of  $L_{POP} \sim 10^7 L_{\odot}$ .

The abscissa can be normalized into a time scale (Lewis & Ibata 2000); the crossing time of an Einstein radius of a Solar mass star is  $9.2 v_{1000}^{-1} h^{-\frac{1}{2}}$  yrs (assuming  $\Omega_o = 1, \Lambda_o = 0$ ), where  $v_{1000}$  is the velocity of the microlensing masses in units of 1000km/s. When considering a population of microlensing objects of a different mass it is only this crossing time that needs to be rescaled, with the degree of fluctuations in Figure 1 remaining the same. Being simply a function of the square root of the lensing masses, if the dark matter in Abell 370 was composed of Jupiter mass compact objects, the corresponding value would be  $\sim 3.5 v_{1000}^{-1} h^{-\frac{1}{2}}$  months.

By combining the light curves from the various stellar samples it is possible to generate a probability distribution for the expected fluctuations (Figure 2). These reflect the features observed in Figure 1, namely that microlensing of lower luminosity populations results in more substantial fluctuations. In terms of integrated probability, a  $10^4 L_{\odot}$  population will exhibit deviations from the mean exceeding 5% for half of all observations. A quarter of all observations will reveal fluctuations exceeding 10%. The corresponding values for the more luminous populations are 2% & 3.5% for  $L_{POP} = 10^5$ , 0.6% & 1% for  $L_{POP} = 10^6$  and 0.2% & 0.3% for  $L_{POP} = 10^7$ . The  $L_{POP} = 10^4 L_{\odot}$  case also displays more extreme fluctuations, experiencing deviations of  $> 15\%$  for 10% of observations, and  $> 29\%$  over 2% of its light curve.

To detect the fluctuations expected for a population of cluster MACHOs it is advantageous to target stellar populations with smaller intrinsic luminosities. Targeting fainter sources, however, presents observational difficulties, such as substantially increased integration times, a point we turn to in the next section.

### 3.2. Observational Considerations

The study of cosmological microlensing by Lewis & Ibata (2000) examined stellar luminosity in a pixel covering a galaxy out to  $z \sim 0.5$ . Here we explore the possibility of using HST to

constrain the microlensing variability in a strongly lensed arc of Abell 370. For a source redshift of  $z = 0.724$ , a spatially resolved population with intrinsic U-band luminosity  $L = 10^7 L_{\odot}$ , magnified by a factor of 8.3, will give rise to an observed V-band flux of 1.3photons/sec/m<sup>2</sup>, ( $\Omega_o = 1, \Lambda_o = 0$ , and  $H_0 = 100\text{km/s/Mpc}$ ). The expected total system efficiency of the new HST instrument the ‘‘Advanced Camera for Surveys’’ is approximately 40% at 6000 Å, so 2.5photons/sec will be detected per  $10^7 L_{\odot}$  population. The sky background will be negligible in comparison, 0.1photons/sec per resolution element (the area encompassed by the point spread function)<sup>1</sup>. In a  $10^4$  sec exposure HST will therefore measure variability to 0.66% accuracy; this would allow a  $3\sigma$  detection of 2% variability events which according to the simulations of §3.1, occur with 0.25% chance. The giant arc in Abell 370 subtends over  $\sim 1000$  HST spatial resolution elements and  $\sim 8$  variability events would be detected in a 2-epoch observation campaign if all the cluster dark matter is in the form of MACHOs. Similarly, for a  $10^6 L_{\odot}$  population, the above  $10^4$  sec integration time would allow 3% variability events to be detected at the  $3\sigma$  level. Approximately  $\sim 100$  such events would be expected in the 2-epoch dataset. Several exposures would be required at each epoch to correct for cosmic rays and to identify Poisson fluctuations in the surface photometry that could be mistaken for microlensing events.

Currently, only coarse surface photometry of the giant arc in Abell 370 has been published, but its total brightness suggests that each HST resolution element corresponds to an average intrinsic source luminosity of  $10^6 \rightarrow 10^7 L_{\odot}$ . HST images of the arc reveals that it is very clumped (Smail et al. 1996) and a range of source luminosities are available for study. We have begun a more detailed modeling of the microlensing in Abell 370, taking into account both the variation in the microlensing parameters and surface brightness over the arc, with the goal of providing a map of the variability signature.

To detect the more common variability in populations of lower luminosity will require NGST. With this instrument, the sky background is ex-

<sup>1</sup>This value was derived from archival WFPC2 ‘‘Planetary Camera’’ data on this cluster.

pected to be substantially lower than on HST:  $< 10^{-1}$  photons/sec/resolution element<sup>2</sup> at  $1.1\mu m$ . Assuming a 20% total system efficiency, a  $10^5$  sec integration at two epochs would allow 10% variability events to be detected at the  $3\sigma$  level in a population of intrinsic luminosity  $10^4 L_{\odot}$ . As discussed above, variability of this magnitude must be very common, occurring in 25% of the resolution elements per epoch. If MACHOs make up a substantial fraction of the dark matter in clusters, giant arcs will be seen to shimmer with NGST, the degree of shimmering being dependent upon the luminosity of the population under consideration.

The above analysis is very encouraging, demonstrating that the signature of microlensing due to cluster dark matter could soon be detected with HST, as well as illustrating that microlensing fluctuations may be ubiquitous in future observations with NGST.

#### 4. Conclusions

If dark matter in galaxy clusters exists in the form of compact objects, it should introduce variability on background sources. Current searches for cluster dark matter have focused upon monitoring quasars behind the Virgo cluster. Its close proximity, however, makes Virgo a poor lens.

By considering clusters at higher redshift, the microlensing optical depth increases, although the potential number of background quasars that can be used as microlensing targets is reduced. In this paper we have examined the microlensing effect that a population of compact dark matter objects would have on the surface brightness distributions of giant luminous arcs. Focusing upon the spectacular arc in Abell 370, numerical simulations reveal that substantial variability can be introduced over the lensed image. This variability is, however, dependent upon the intrinsic luminosity of the population of stars under consideration, with more luminous populations displaying more quiescent light curves.

To detect microlensing induced variability in the surface brightness of the giant arcs, a deep monitoring program over a single semester is required. Such a program would allow easy identi-

cation of variability contaminants, such as novae, supernovae and highly luminous variable stars, due to their characteristic temporal profiles (see Lewis & Ibata 2000). These contaminating systems are also rare, while microlensing variability will appear ubiquitously over the arc. As the mass distribution in the cluster can be determined via the modeling of the macrolensing features, the identification of microlensing variability will reveal the MACHO mass fraction within the cluster. Many strongly lensed systems are available for study, several displaying very extended structure [e.g. cB58 (Yee et al. 1996)], providing ideal tools for the examination of the nature of cluster dark matter.

#### Acknowledgments

GFL thanks the computer support and staff at the Anglo-Australian Observatory for providing the facilities on which the simulations presented in this paper were undertaken.

#### REFERENCES

- Abdelsalam, H.M., Saha, P. & Williams, L.L.R. 1998, MNRAS, 294, 734
- Afonso, C. *et al.* 1999, A&A 344, 63
- Alcock, C. *et al.* 1999a, ApJ, 521, 602
- Alcock, C. *et al.* 1999b, ApJS, 124, 171
- Alcock, C. *et al.* 2000a, astro-ph/0001272
- Alcock, C. *et al.* 2000b, astro-ph/0002510
- Ansari, R. *et al.* 1999, A&A, 344, L49
- Bird, C. M., Dickey, J. M. & Salpeter, E. E. 1993, ApJ, 404, 81
- Crotts, A.P.S. 1992, ApJ, 399, L43
- Fort, B. & Mellier, Y. 1994, ARAA, 5, 239
- Gould, A. 1995, ApJ, 455, 44
- Henry, J. P., Briel, U. G. & Nulsen, P. E. J. 1993, A&A, 271, 413
- Hodgkin, S. T., Oppenheimer, B. R., Hambly, N. C., Jameson, R. F., Smartt, S. J., Steele, I. A. 2000, Nature, 403, 57

<sup>2</sup>see <http://www.ngst.stsci.edu/sky/sky.html>

- Ibata, R.A., Irwin, M.J., Bienaymé, O., Scholz, R. & Guibert, J. 2000, ApJ, 532, 41L
- Jahreiß H. & Wielen, R. 1997, in: B. Battrock, M.A.C. Perryman and P.L. Bernacca (eds.): HIPPARCOS '97. Presentation of the Hipparcos and Tycho catalogues and first astrophysical results of the Hipparcos space astrometry mission, Venice, Italy, 13-16 May(1997; ESA SP-402, Noordwijk, p.675-680
- Klypin, A., Kravtsov, A. V., Valenzuela, O. & Prada, F. 1999, ApJ, 522, 82
- Kneib, J.-P., Mellier, Y., Fort, B. & Mathez, G. 1993, A&A, 273, 367
- Lasserre, T. *et al.* 2000, A&A, 355, L39
- Lewis, G.F. & Ibata, R.A. 2000, ApJ, *In Press*
- Lewis, G.F. & Irwin, M.J. 1995, MNRAS, 276, 103
- Lewis, G.F. & Irwin, M.J. 1996, MNRAS, 283, 225
- Lewis, G.F., Miralda-Escude, J., Richardson, D.C. & Wambsganss, J. 1993, MNRAS, 261, 647
- Smail, I., Dressler, A., Kneib, J., Ellis, R. S., Couch, W. J., Sharples, R. M. & Oemler, A. J. 1996, ApJ, 469, 508
- Soucail, G., Fort, B., Mellier, Y. & Picat, J. P. 1987, A&A, 172, L14
- Soucail, G., Mellier, Y., Fort, B., Mathez, G. & Cailloux, M. 1988, A&A, 191, L19
- Tadros, H., Warren, S.J. & Hewett, P.C. 1988, New Astr., 42, 11
- Tadros, H., Warren, S.J. & Hewett, P.C. 2000, astro-ph/0003422
- Walker, M. A. & Ireland, P. M. 1995, MNRAS, 275, L41
- Witt, H.-J. 1993, ApJ, 403, 530
- Wyithe, J. S. B. & Webster, R. L. 1999, MNRAS, 306, 223
- Wyithe, J. S. B., Webster, R. L. & Turner, E. L. 1999, MNRAS, 309, 261
- Wyithe, J. S. B., Webster, R. L. & Turner, E. L. 2000, MNRAS, 312, 843
- Yee, H. K. C., Ellingson, E., Bechtold, J., Carlberg, R.G. & Cuillandre, J.-C. 1996, AJ, 111, 1783

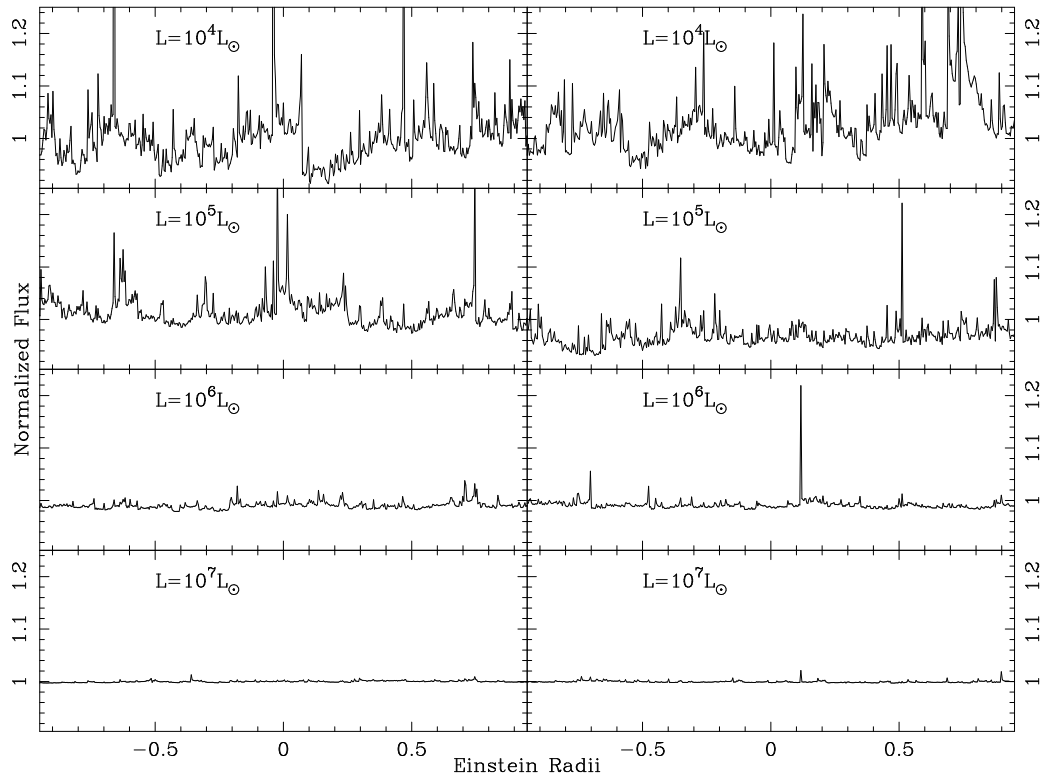


Fig. 1.— Two sets of examples of light curves for various stellar populations. The abscissa is in units of Einstein radii, while the ordinate presents the fluctuations with respect to the mean. Both sets display the same general trends that are seen in all the light curves. Namely, that the lower luminosity stellar populations show the most rapid variability. As the total luminosity of the population is increased, even luminous stars that are strongly lensed contribute only small variations to the light curve.

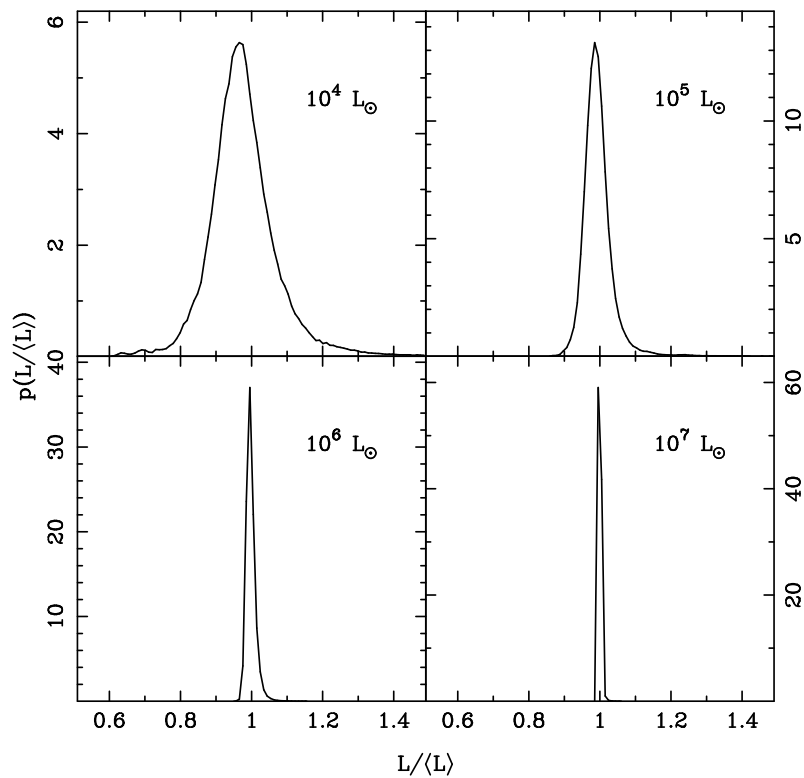


Fig. 2.— The fluctuation probability distributions for the populations with intrinsic luminosities of  $10^4, 10^5, 10^6$  and  $10^7 L_\odot$ . Note that the observed luminosity is  $L_{Obs} = \langle \mu_{th} \rangle L_{POP}$  and the different ordinate scaling on each panel. As expected from the light curves presented in Figure 1, the lower luminosity populations show a broad distribution, which narrows as the total luminosity is increased.